E-Journal of Advanced Maintenance Vol.11 No. 4 (2020) 163-171
Japan Society of Maintenology

Applicability of ultrasonic-wave based method for integrity assessment of concrete severely damaged by heat

Vu Nhut LUU[1,3*], Kenta MURAKAMI[1], Thi Mai Dung DO[1], Masahide SUZUKI[1], Tomonori YAMADA[2], Takuya SHIBATA[2], Hiroyuki DAIDO[2]

[1] *Nagaoka University of Technology, Kamitomioka 1603-1, Nagaoka, Niigata, 940-2188, Japan*
[2] *Japan Atomic Energy Agency, Nakamaru 1-22, Yamadaoka, Naraha-machi, Futaba-gun, Fukushima, 979-0513, Japan*
[3] *Vietnam Atomic Energy Institute (VINATOM), 59 Ly Thuong Kiet, Hoan Kiem, Hanoi, Viet Nam*

ABSTRACT

Previous studies on the effect of temperature on various types of concrete have been mainly focused on the case of fire in which the exposure duration is short. Limited data has been obtained regarding the effect of high temperature on concrete properties under severe accident condition in which the concrete structure may be exposed to heat radiation from melting nuclear fuels for a long time. The present study aimed to examine the applicability of the ultrasonic wave-based method for concrete damaged extremely by heat simulating a severe accident. The conventional ultrasonic test was conducted in concrete cylindrical with the size of ϕ 100 × 200 mm after exposure to high temperatures 105, 200, 400, 600, 700, 800 °C. The results revealed that this method is sensitive to indicate thermal damage as results from water content loss and decomposition of portlandite. A strong correlation between dynamic and static elastic modulus was obtained for concrete exposed to temperature range of 25 to 400 °C, corresponding to dynamic elastic modulus range from 20 - 40 GPa. The degradation within this range is due to water loss. At higher temperatures, the concrete integrity is not maintained due to the formation of cracks and the decomposition of cement paste phases, which cause a significant decay of the ultrasonic waves.

KEYWORDS

Severe accident, integrity assessment, attenuation, dynamic elastic modulus, P-wave, S-wave.

ARTICLE INFORMATION

Article history:
Received 06 December 2018
Accepted 31 January 2020

Introduction

In the construction of nuclear facilities, concrete has been used as a structural material in radiation shielding walls and pedestals that may be exposed to a high temperature during a severe accident. It is important to assess the integrity of structures after a severe accident, where concrete is exposed to a high temperature for the long duration. Since the studies on the influence of temperature on various types of concrete used in civil construction have been mainly focused on the case of fire in which the exposure duration is short. This research aims to provide basic information for developing a remote nondestructive test method using laser-induced ultrasonic waves [1] for application in the assessment of the structural integrity of concrete pedestals after a severe accident in the Fukushima Daiichi Nuclear Power Plants. For this purpose, the conventional ultrasonic wave technique using direct transmission was employed to investigate the degree of damage caused by heat treatment.

Concrete is a composite material including aggregates and cement paste which has complex water-containing phases. These phases are vulnerable to high temperature exposure due to water loss. When concrete is exposed to high temperatures, various irreversible reactions take place and the mechanical properties such as strength degrade significantly [2–5]. The major effect is the decomposition of water-containing phases in cement paste, such as ettringite, portlandite ($Ca(OH)_2$), and calcium-silicate-hydrate, so-called C-S-H gel. The first decomposition in concrete is ettringite, occurring early below 100°C. Then, capillary water escapes in conjunction with dehydration of C-S-H

*Corresponding author, E-mail: nhut.czech@gmail.com

gel in the temperature range of 100°C – 500°C. When the temperature reaches between 400 - 600°C, the portlandite starts to decompose. Beyond 600°C, β-C_2S (β-dicalcium silicate) is formed by the decomposition of C-S-H gel [5−6].

Ultrasonic-wave based method is widely utilized in detecting the discontinuities and damage in various types of material. Ultrasonic wave propagation in solids normally consists of three components: (1) longitudinal wave in which the particle moves in the same direction of propagation, so-called *P-wave* velocity and (2) shear wave in which the particle moves perpendicular to the direction of propagation, so-called *S-wave* velocity, and (3) surface wave (which will not be discussed in this study because we used direct pulse transmission technique) [7]. The P-wave has been commonly applied to monitor the scalar damage in concrete caused by heat [2–4]. Using this technique, the internal change in concrete can be identified by measuring the change of velocity through the material. Handoo et al. (2002) showed that P-wave velocity was significantly reduced within the range of 300°C and 700°C, and the pulse did not pass through the samples at 800°C due to high crack density formation [4]; Chu et al. (2016) also reported, after 600°C the variation of velocity is small, and it does not change much in the range of 800 – 1000°C [3]. On the other hand, S-waves are likely sensitive to the matrix connectivity [8] and can also be used to monitor the internal change in concrete subjected to high temperature. However, the use of S-waves for characterizing the internal change in concrete is rare because the major difficulty is to estimate the rising instance of the signal since P-waves has higher velocity than S-waves [7] and arrives sooner at the receiving transducer. This leads to misestimating of the onset of S-waves because P-waves and S-waves overlapped and therefore become difficult to differentiate.

Elastic modulus is a basic parameter for evaluating the deformation and integrity of structural components. In the existing structure, core extraction test is commonly used to provide information on the elastic properties of concrete. However, this technique seems to have limitations in the case of severe accidents due to high radiation risk. Alternatively, elastic modulus can be determined from dynamic elastic modulus, which is calculated from ultrasonic pulse velocities. In this method, both P-wave and S-wave velocity is required for the calculation (according to ASTM C 597). Recently, a new method using Hilbert transformation has been introduced [9] which was employed in this study for determining the onset of S-waves on concrete. This study attempted to monitor the variation in concrete after high-temperature exposure using both P-wave and S-wave transducers in order to identify the temperature range between which the ultrasonic-based techniques may be applied to monitor concrete structures after a severe accident.

2. Material and experiments

The concrete specimens (ϕ 100 × 200 mm) were prepared. The mixture proportions per cubic meter were 157 kg of water, 285 kg of sand (fine aggregates), 838 kg of coarse granite aggregate with water/cement ratio of 0.55. The admixture of 1% was also added. The specimens were cured for 28 days, and then placed in ambient air before the compressive test. The heat treatment was carried out in electric furnace. The temperature gradient was controlled by measuring the temperature of furnace and specimen cores, which were measured by representative specimens with an embedded thermocouple during concrete preparation. The holding time and heating rate was set to make a uniform damage within specimen cross-section. The detail of heat treatment conditions is shown in Table 1.

The conventional ultrasonic test was employed using a pulse generating-receiving device (OLYMPUS 5077PR) connected to an oscilloscope (TEKTRONIX DPO2022B), which acquires waveforms. The experimental setup is a simple direct-transmission ultrasonic configuration as shown in Fig.1. Velocity measurements were carried out using both, a P-wave transducer with a diameter of 50 mm and S-wave transducer with a diameter of 25 mm. Both transducers have a center frequency of 100 kHz. Before taking measurements, the travel time between transmitting and receiving transducers without specimen was measured, which was about 0.44 μs and 0.32 μs for the P-wave and S-wave transducer, respectively. In this experiment, the transducers were placed at the top and bottom surface of a cylindrical sample. The path length of wave propagation (L) is about 200 mm. Knowing the path length, the P-wave and S-wave velocity (V_p and V_s, respectively) can be calculated from the travel time (Δt), V_p or $V_s = L/\Delta t$. Then these velocities were used to calculate the dynamic elastic modulus of elasticity E_d by Eq. (1) according to ASTM C 597:

$$E_d = \frac{\rho V_d^2 (1+\upsilon_d)(1-2\upsilon_d)}{(1-\upsilon_d)}; \upsilon_d = \frac{1-2(V_s/V_p)^2}{2-2(V_s/V_p)^2} \quad (1)$$

where ρ is the concrete density, v_d is the dynamic Poisson's ratio. Hilbert transformation is used to obtain the envelope of the waveform by which the onset of S-wave propagation can be distinguished from that of the P-wave [9]. The transformation was done with a MATLAB code using the syntax, *y = hilbert (xr),* which returns the analytic signal, y, from a real data sequence, *xr*, and then each element of *y* was returned to the absolute value with the function, *abs* (*y*).

Table 1 Heating and cooling conditions of concrete specimens

Target temp. (°C)	Monitoring location	Heating rate (°C /min)	Cooling rate (°C /min)	Holding time (hours)
105	Furnace	0.9	0.11	504
	Specimen core	0.48	0.12	
200	//	0.92	0.31	336
	//	0.48	0.28	
400	//	0.65	0.68	24
	//	0.64	0.71	
600	//	0.64	0.69	16
	//	0.63	0.69	
700	//	0.71	0.77	16
	//	0.68	0.72	
800	//	0.73	0.80	6
	//	0.73	0.79	

The compressive test was conducted on a universal hydraulic test machine; the static elastic modulus was calculated according to Japanese Standard JIS A1149 - 2001. To confirm the change in chemical composition, X-ray diffraction (XRD) tests using a Rigaku's X-ray diffractometer Miniflex 600 with Cu Kα radiation (λ = 1.54056 Å, operating at 40 kV and 15 mA) were carried out, the samples for XRD tests were collected from broken pieces from the compressive test, and then they were ground to fine grain size and sieved using a hand sieve with nominal grid size of 75 µm.

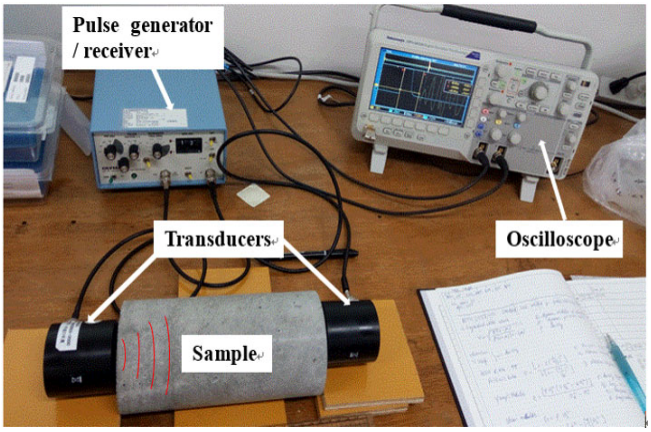

Fig. 1.Test arrangement for the conventional ultrasonic test

3. Results and discussion

3.1. Degradation of concrete by heat

Fig.2 shows the effects of temperature on weight loss. The weight loss was calculated from the weight before and after heating. In the range of 25 - 105°C, concrete lost weight rapidly due to the releasing of water in the capillary pores. Between 105°C and 400°C, the change in weight is negligible

because most of water was lost at 105°C, and only physically bound water in fine pores of C-S-H gel may be dehydrated [6]. After 400°C, the loss continued gradually due to the loss of chemically bound water in water-containing phases, including portlandite and C-S-H gel. The loss was about 4% and 8% after exposed to 400°C and 800°C, respectively.

By observing the surface condition, no spalling (surface failure caused by internal pore pressure) occurred after heat treatments, and the concrete remained intact up to 800°C. However, color changes and formation of cracks can be observed on the concrete surface (Fig.3). At 105°C, no visible cracks are observed. At 200°C, a few visible cracks were detected, and they became pronounced in both size and density from 400°C up to 800°C. On the other hand, the color of concrete did not change when being heated to 200°C. At 400°C, it turned red and then turned whitish-grey between 600°C and 800°C. This phenomenon may be related to the change in chemical composition.

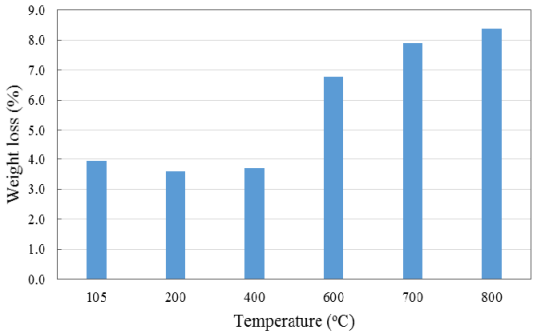

Fig. 2. The change of weight at different exposure temperatures

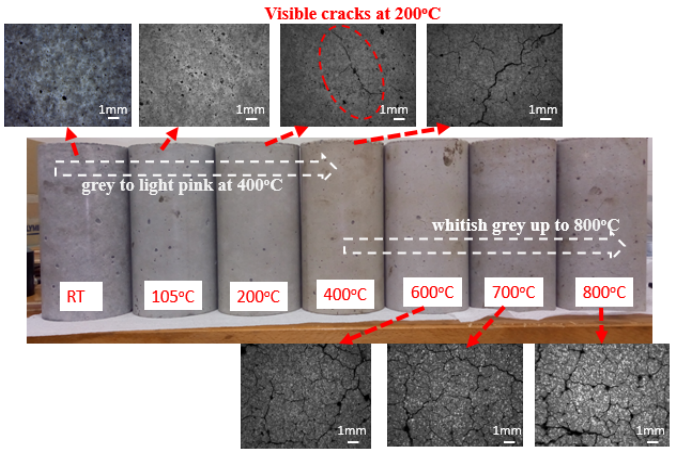

Fig. 3. Variation of concrete surface at different exposure temperatures

Fig. 4 presents the XRD diagram for the samples with various temperature exposures. At the initial stage, four crystalline phases can be identified, including quartz (SiO_2), albite (coming from aggregates), portlandite ($Ca(OH)_2$ with d = 2.4 Å) and unhydrated <C_3S (tricalcium silicate) and β-C_2S> (with d = 2.6 - 2.8 Å corresponding to 2θ angles between 32 and 33°). It should be noted that it is difficult to distinguish between the peaks of β - C_2S and C_3S because their peaks have similar structure and diffraction angles [10]. In addition, the main hydrated phase, C-S-H gel cannot be indexed due to its amorphous nature, although C–S–H gel occupied about 60% of the cement paste [11]. It can be seen that almost no chemical decomposition of cement paste phases occurred below 400°C, while the peak of $Ca(OH)_2$ was reduced after 400°C. Between 700°C to 800°C, the peak intensity of < β-C_2S + C_3S > was intensified obviously. This is probably due to the transformation of the amorphous C-S-H phase into β-C_2S phase, which is a crystalline phase, which is consistent with previous reports [5 - 6]. However, the peak of α-quartz was persistent up to 800°C, and we could not detect the β-quartz in the XRD patterns beyond 600°C even though there is an α - β transition in quartz at 573°C [6], [12].

Fig. 5 illustrates the change of mechanical properties of concrete that was exposed to different temperatures. The strength and modulus of elasticity had similar behaviors, which decreased

continuously as temperature increased. The compressive strength of the unheated sample was about 41.8 MPa but suffered a significant reduction after exposures. For example, the residual strength remained about 75% of its original strength at 105°C, 43% at 400°C and 22.8% at 600°C. When concrete was heated to 800°C, only 13.3% of strength remained. Regarding the structural integrity, although after 336 hours heated to 200°C, the residual strength remained at about 25 MPa. This suggests that below 200°C, concrete still retains integrity in term of the design strength (about 22 MPa [13]).

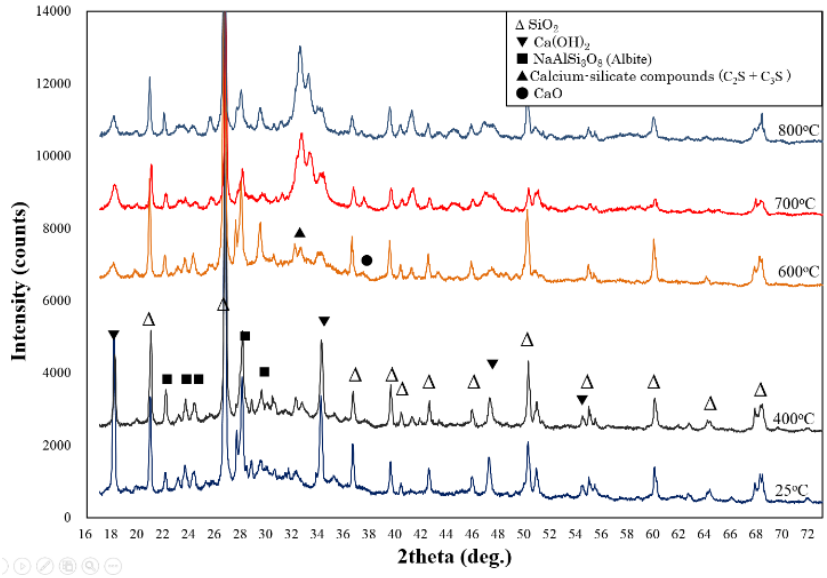

Fig.4. Variation of chemical composition by using XRD

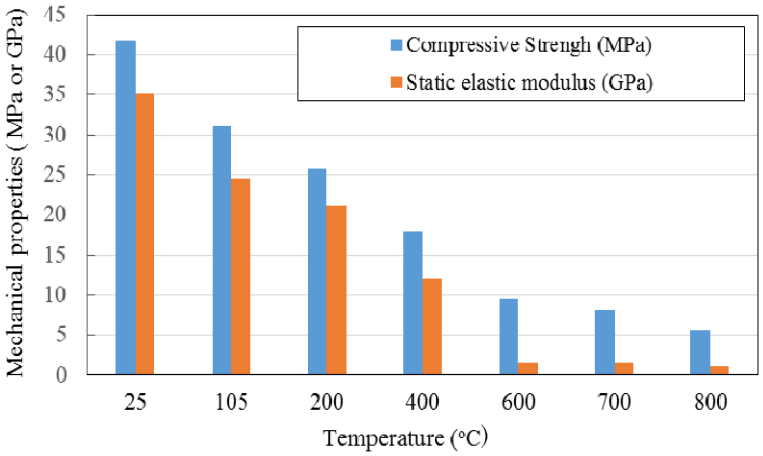

Fig.5. The mechanical properties of concrete at different exposure temperatures

3.2. Variations of ultrasonic parameters

Fig.6 shows the time-dependent signals obtained for thermal damage in concrete. Generally, the amplitudes of the waveforms decayed as exposure temperature increases. It can be seen that S-waves showed higher attenuation than P-waves at the temperature range of 25 – 200°C. This suggests S-waves are a better indicator of thermal damage due to capillary water loss than P-waves since they are more sensitive to matrix connectivity [8]. Beyond 200°C, amplitudes of both S- and P-waves decreased rapidly and became saturated between 600 and 800°C. In this temperature range, the signals can only be observed if magnified to 40dB (or 100 times enhanced), which indicate heavy damage in the concrete structure. Since the energy of the ultrasonic wave can be represented as the amplitude of the signal, as the level of damage increases, lower amplitude results from energy absorbed by the

damaged concrete due to scattering and dispersion on scatterers (cracks or pores). This process redistributes the energy of the incident wave in all direction, and only a small amount of energy can remain in the forward direction that can reach the receiving transducer [14]. Fig. 6c gives the Hilbert transformation of the raw signals. The obtained envelope of the waveforms is able to distinguish the onset of S-wave and P-wave propagation. The first interruption indicates the onset of P-waves, as P-waves are the fastest among ultrasonic velocity components, while the second interruption indicates the onset of S-wave propagation. The onset times for S-waves were then used to calculate the S-wave velocities.

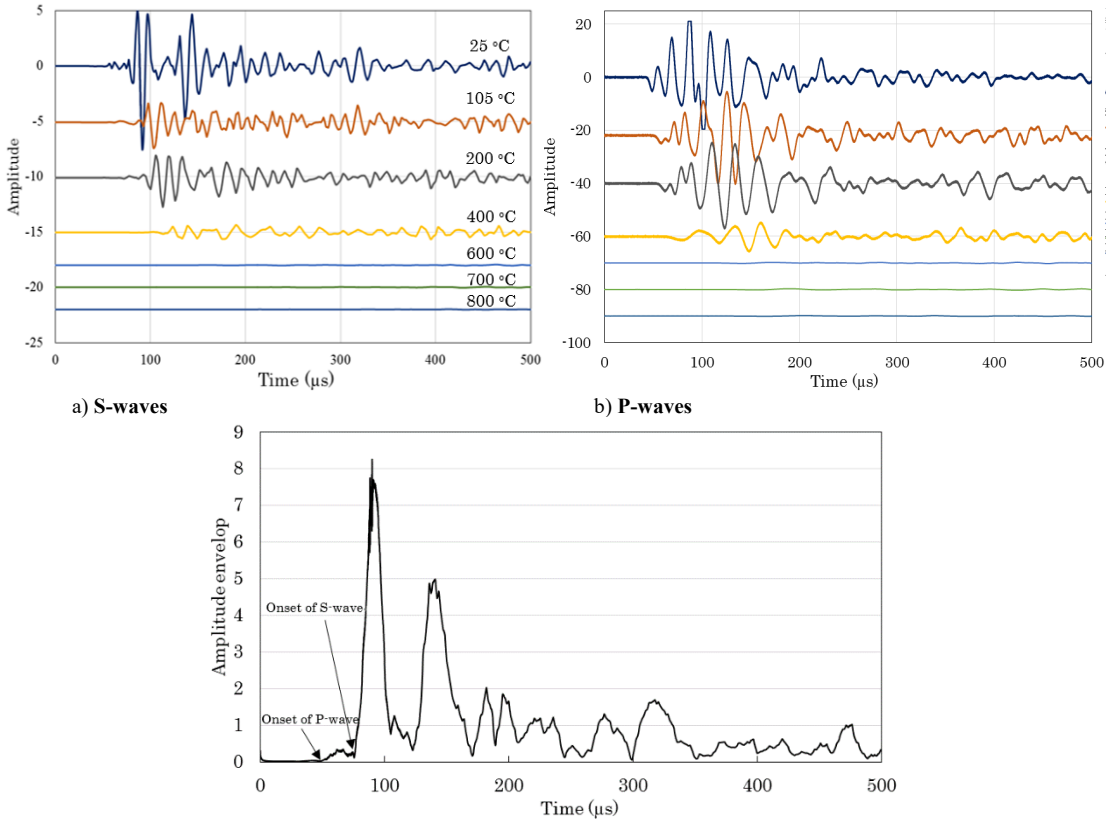

a) **S-waves** b) **P-waves**

c) **Representative transformed signals of raw S-wave for unheated concrete**

Fig.6. Time dependent signals at different exposure temperatures

Fig.7 presents the result of velocities of concrete before and after heating at high temperatures. For S-waves, it was possible to determine the rising instance when concrete was exposed up to 400°C. Beyond this, the signal is not stable due to high attenuation of the wave energy, with the reduction by > 98% of amplitude compared to that in unheated concrete. Since the vibration of particles in S-waves is perpendicular to the direction of propagation, it is very sensitive to cracks when the crack faces are perpendicular to the propagation direction. In this case, high density of surface cracks above 400°C could be associated with the reduction of S-wave velocity. In contrast, the rising time of P-waves was measurable up to 800°C. As seen in Fig.7, the velocities decreased continuously with the increasing temperatures. A rapid decrease was observed at 105°C (-15.5%) and between 400 - 600°C (-31.2% at 400°C and -61.5% at 600°C), this could be associated with the releasing of capillary water and decomposition of portlandite, respectively. Particularly, between 600°C and 800°C, the variation of pulse velocities was negligible; this is similar with the evolution of static elastic modulus. This suggests the saturation of degradation above 600°C.

The propagation of ultrasonic waves depends on the physical state of concrete. When concrete has integrity, the travel time required for wave to reaches the receiving transducer is shorter compared to that after subjected to high temperature. Though numerous variables influence the speed in ordinary concrete[7], microcracks and water content would be contribute dominantly in this case. As a consequence of thermal damage, the porosity increases due to water loss, and formation of

microcracks due to the deformation caused by the mismatch between contraction of cement paste and expansion of aggregates [5],[15], and this may contribute to reducing the incident wave energy and extending the traveling time, resulting in a reduction of velocity. We propose that the water loss mainly contributes to degradation of both mechanical properties and wave velocities below 400°C, while crack formation due to decomposition of hydrated products is dominant beyond 400°C, as follows:

- At 105°C, the evaporation of water in capillary pores and dehydration of C-S-H occurs; the velocity is influenced by the decrease of water content in pore structure, which is confirmed by weight loss.
- Between 105 - 400°C, the C-S-H gel dehydrates strongly [6]. Zhang et al. (2013) proposed that the interlayer water, which exists in the globulus C-S-H, is released partially but the globulus structure is not affected [16]. Because of the small amount of interlayer water releasing, it does not influence on weight loss. However, this small change also affects the wave propagation because the fine pores in the matrix would affect the vibration of particles.
- Between 400 - 600°C, weight loss increases obviously due to the decomposition of portlandite by releasing the crystal water ($Ca(OH)_2 \rightarrow CaO + H_2O$). Because the aggregate surface is covered by a layer of portlandite [17], the decomposition may cause cracking around the perimeter of aggregates. The cracks in this interface can appear at 350°C and more severely at 550°C due to decomposition of portlandite [15]. Thus, microcracks may have a dominant effect on velocity reduction beyond 400°C.
- Above 600°C, the amorphous C-S-H gel is transformed into small crystalline β - C_2S and it can lead to a reduction of the volume of C-S-H significantly [16]. This phenomenon was confirmed by XRD by the increase of β-C_2S peak intensity. On the other hand, the siliceous aggregates (sand) expands 5% in the volume due to the α - β quartz transition [12]. These concurrent phenomena may lead to form cracking not only in the interface between aggregates and paste but also inside the aggregates.

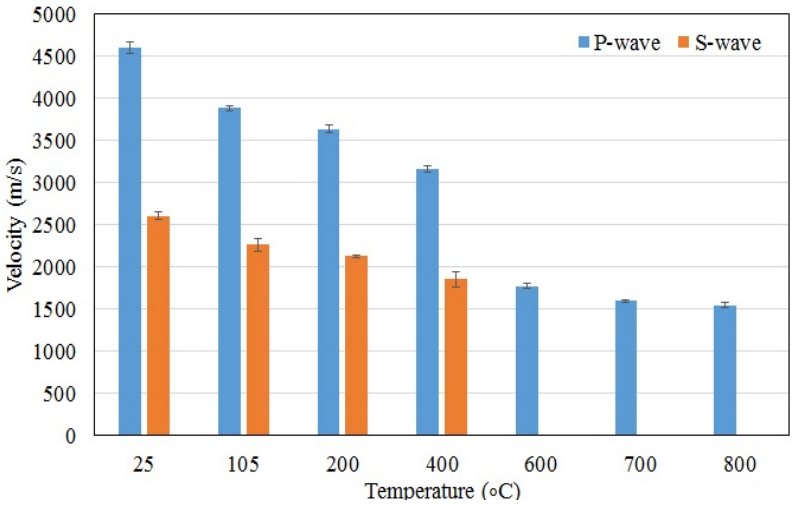

Fig.7. The variations of velocities in concrete at different exposure temperatures

3.3. Correlation between dynamic and static elastic modulus

The estimation of in situ structural integrity requires elastic modulus of concrete; this parameter can be determined by compression test, so called static elastic modulus. The values are used to correlate with the dynamic elastic modulus calculated from the ultrasonic velocities. Thus, the information on elastic modulus can be roughly estimated based on this correlation.

Due to high decay of S-waves beyond 600°C, the velocity was difficult to determine, and the dynamic elastic modulus, E_d after this temperature cannot be computed. This highlights the limitation of ultrasonic wave measurement techniques for the estimation of elastic modulus in concrete heavily damaged by heat. However, this technique can be used to locate the most damaged area based on the

loss of ultrasonic wave energy, which is in the form of amplitude. Fig. 8 presents the obtained relationship between the static elastic modulus (E_s) calculated from the stress-strain curve obtained by compression test using JIS A 1149-2001 and the dynamic elastic modulus (E_d) calculated from ultrasonic wave velocities using ASTM C 597. This correlation has the coefficient of determination R^2 near 1 ($R^2 = 0.98$) for concrete samples after heat treatment up to 400°C, corresponds to E_d which varies from about 20 to 40 GPa, as given by the Eq. (2):

$$E_s = 1.08E_d - 7.11 \quad (2)$$

As can be seen, E_d has a linear relationship with E_s , but the meaning of the obtained dynamic elastic modulus is generally higher than the static elastic modulus, which is about 12%. However, the obtained values are considered to be reasonable for this technique [7]. The different between E_d and E_s is because of the non-linear stress-strain behavior in concrete which is associated with the different frequency between two loading conditions, resulting higher frequency leads the larger elastic modulus [18]. In the compression test, static elastic modulus is determined by the dynamic test at a very low frequency, such as, testing duration in 5 minutes corresponding 3.3 x 10^{-3} Hz, while dynamic elastic modulus is determined at high frequency, in this case, is 100 kHz. Therefore, the stress-strain behavior is apparently different.

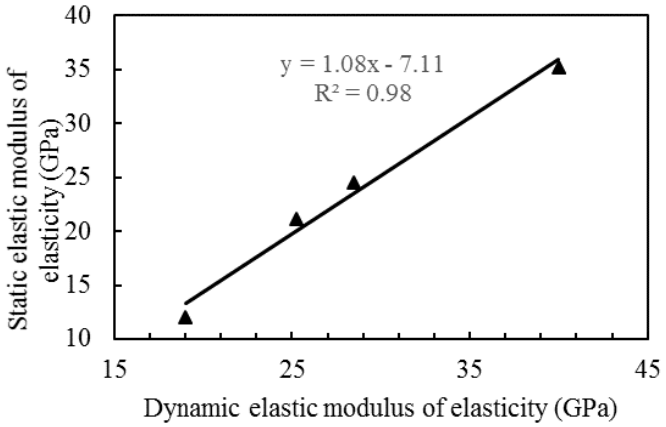

Fig. 8. Correlation between static and dynamic elastic modulus

4. Conclusion

- When concrete is subjected up to 800°C, the degradation can be clarified into two types: water loss-dominated degradation below 400°C and decomposition-dominated degradation beyond 400°C:
  (1) At 105°C, due to long time exposure, the strength, modulus of elasticity and velocity reduced significantly. The mechanism is associated with the evaporation of capillary water. Between 105 and 400°C, the weight was almost not changed, but strength and elasticity continued to degrade. During this temperature exposure, the bound water in hydrated products is released, but due to the very fine structure change, it has a negligible effect on the weight. In contrast, the water release had a great impact on mechanical properties and velocity.
  (2) The surface cracks are very pronounced after 400°C, the loss of strength and ultrasonic velocity was gradual. Between 600°C to 800°C the concrete lost over 80% of its original strength, and the change in strength and ultrasonic velocity became saturated. The C-S-H structure may be dramatically decomposed due to the phase transformation into β-C_2S.
- The ultrasonic wave measurement method is sensitive to thermal degradation especially for damage caused by water content loss and the decomposition of portlandite at 105°C and between 400 to 600°C, respectively. S-waves are better indicator of thermal damage than P-wave, resulting from water loss below 200°C.

- A strong correlation between dynamic and static elastic modulus was obtained for concrete exposed to temperature range of 25 to 400°C, corresponding to dynamic elastic modulus range from 20 - 40 GPa. Within this range, laser ultrasonic can be utilized to monitor damaged caused by water loss. After 400°C, concrete is severely damaged due to the formation of crack and the decomposition of cement paste phases, which cause the significant decay of the ultrasonic wave, thus laser ultrasonic method is not suitable.

Acknowledgment

This study was supported by the Japan Atomic Energy Agency**.**
The authors would like to express their thanks to Prof. Takumi Shimomura of Nagaoka University of Technology for his kindness to share the mechanical test equipment to this study.

References

[1] T. Yamada, H. Suzuki, T. Hanari, T. Shibata, A. Nishimura, S. Koyama, H. Daido, Y. Shimada, O. . Kotyaev, and S. Kurahashi, "Evaluation of concrete strength by laser induced ultrasonic waves," presentation in The Japan Atomic Energy Society Fall 2016, 2016.
[2] Y. Sato, D. Thi-mai-dung, and M. Suzuki, "Study on Material Properties of Concrete Structures Exposed to Extremely High Temperature due to Severe Accident," E-Journal Adv. Maint., vol. 9, no. 3, pp. 164–166, 2017.
[3] H. Chu, J. Jiang, W. Sun, and M. Zhang, "Thermal behavior of siliceous and ferro-siliceous sacri fi cial concrete subjected to elevated temperatures," Mater. Des., vol. 95, pp. 470–480, 2016.
[4] S. K. Handoo, S. Agarwal, and S. K. Agarwal, "Physicochemical, mineralogical, and morphological characteristics of concrete exposed to elevated temperatures," Cem. Concr. Res., vol. 32, no. 7, pp. 1009–1018, 2002.
[5] I. Hager, "Behaviour of cement concrete at high temperature," Bull. Polish Acad. Sci. Tech. Sci., vol. 61, no. 1, pp. 145–154, 2013.
[6] D. Naus, "The Effect of Elevated Temperature on Concrete Materials and Structures — A Literature," Oak Ridge National Laboratory, 2005.
[7] V. M. Malhotra and N. J. Carino, Handbook on Nondestructive Testing of Concrete. 2004.
[8] J. Carette and S. Staquet, "Monitoring the setting process of mortars by ultrasonic P and S-wave transmission velocity measurement," Constr. Build. Mater., vol. 94, pp. 196–208, 2015.
[9] R. Birgül, "Hilbert transformation of waveforms to determine shear wave velocity in concrete," Cem. Concr. Res., vol. 39, no. 8, pp. 696–700, 2009.
[10] G. F. Peng and Z. S. Huang, "Change in microstructure of hardened cement paste subjected to elevated temperatures," Constr. Build. Mater., vol. 22, no. 4, pp. 593–599, 2008.
[11] P. K. Mehta and P. J. M. Monteiro, Concrete: microstructure, properties, and materials. 2006.
[12] P. E. Grattan-Bellew, "Microstructural investigation of deteriorated Portland cement," Constr. Build. Mater., vol. 10, no. 1, pp. 3–16, 1995.
[13] TEPCO, "Technical Strategic Plan 2017 for Decommissioning of the Fukushima Daiichi Nuclear Power Station of Tokyo Electric Power Company Holdings, Inc.," 2017.
[14] T. Shiotani and D. G. Aggelis, "Wave propagation in cementitious material containing artificial distributed damage," , Materials and Structures vol. 42, pp. 377–384, 2009.
[15] E. Annerel and L. Taerwe, "Revealing the temperature history in concrete after fire exposure by microscopic analysis," Cem. Concr. Res., vol. 39, no. 12, pp. 1239–1249, 2009.
[16] Q. Zhang, G. Ye, and E. Koenders, "Investigation of the structure of heated Portland cement paste by using various techniques," Constr. Build. Mater., vol. 38, pp. 1040–1050, 2013.
[17] S. Diamond, "The microstructure of cement paste and concrete - A visual primer," Cem. Concr. Compos., vol. 26, no. 8, pp. 919–933, 2004.
[18] M. Ciccotti and F. Mulargia, "Differences between static and dynamic elastic moduli of a typical seismogenic rock," J. Int. 157, pp. 474–477, 2004.